

Željka Lučev Vasić¹, Yueming Gao², Min Du², Mario Cifrek¹

INTRABODY COMMUNICATION RESEARCH

¹ University of Zagreb, Faculty of Electrical Engineering and Computing

² Fuzhou University, College of Physics and Information Engineering

Intrabody communication (IBC) is a new type of wireless communication, in which the human body, together with its immediate environment, becomes a part of a communication channel. IBC systems exploit the electrical properties of the human tissues for the transmission of signals between various wireless electronic devices (transmitters and receivers) placed on the surface of the skin, in its vicinity, or implanted inside the user's body [1-4]. Such devices can be health monitoring devices (heart rate, blood pressure, or body temperature monitors), sensors of physiological signals (electrocardiogram, ECG; electromyogram, EMG; electroencephalogram, EEG), biomedical implants (pacemakers, hearing devices, endoscopic capsules), or devices for assisted living. Typically, communication between wireless devices is accomplished using standard wireless communications, such as Wi-Fi, Bluetooth, Bluetooth Low Energy, RFID, NFC, ZigBee. However, standard wireless communications have not been designed to be used in the vicinity of the human body - they have been optimized for other applications and have either high power consumption, safety issues, or low data rates. As their alternative in the vicinity of the human body, intrabody communication has been proposed. IBC limits the communication range to the user's body, operates at lower frequencies and lower distances than standard wireless systems and accordingly have lower power consumption. Due to the reduced power consumption, heating and tissue irritation of the users are lower, and the battery lifetime is longer. Using IBC also provides an inherent security mechanism: since the communication signal is dominantly confined to the human body, it is difficult to intercept and eavesdrop.

Two main methods of intrabody communication are galvanic and capacitive coupling. In a galvanic coupling method electrodes of IBC devices are in direct contact with the human body. A single signal differential path is established through a current flow that penetrates into internal tissues. In capacitive coupling, a forward signal path is established through the human body and a return path is formed through the environment. This feature allows the interconnection of devices that are both deployed on the same body surface or close to it, without the need for direct contact with the skin. The capacitive method allows higher achievable data rates and lower path loss compared to the galvanic IBC method, especially for higher communication distances on the

body. It has been shown recently that a stable capacitive return path can be accomplished even in implantable devices, in case the ground electrode is isolated from the human tissue [4-9]. In [10] the authors analysed compliance of the current density and electric/magnetic fields generated in different modalities of IBC with the established safety standards using the circuit and FEM based simulations. The results show the currents and fields in the capacitive IBC system are orders of magnitude smaller than the specified safety limits. However, galvanic HBC with differential excitation at the wrist can result in localized current densities and field intensities around the electrode, which are significantly higher than the safety limits. They also carried out a small *in vivo* study of vital parameters monitoring using capacitive IBC and the acquired data statistically showed no significant change in any of the vital parameters of the subjects.

The transmission characteristic of an IBC system depends on the properties of tissue and a signal path, which is defined by the signal transmission method, location of the transmitter relative to the receiver, environment configuration, signal amplitude, carrier frequency, and type of modulation. The selection of the appropriate carrier frequency in IBC arises from a trade-off between several factors, like a type of signal coupling, safety regulations to avoid interference with common biological signals, specifications of very low consumption and high tissue conductivity, external noise, and so forth. As opposed to standard wireless systems, which require antennas for communications, IBC systems require only small electrodes. Signal and ground electrodes can be connected to the body, but they can also be left floating, depending on the signal frequency, coupling technique, and application [4].

The latest state of technology related to intrabody communication was published in review papers in 2018 [2] and 2020 [4]. IBC research directions of the research group are IBC channel characterization by means of *in vivo* measurements and modelling, and the development of IBC prototype devices for a specific application.

Measurements of IBC channel characteristics

In intrabody communication many overlapping physical mechanisms occur at the same time, making channel

characterization and measurements a challenging task. In addition to this, IBC channels change dynamically with electrode positions and size, subject, subject's movements, and surrounding environment.

Establishing a proper procedure and measurement setup for measuring IBC channel characteristics, while keeping the overall IBC signal path intact, is a very challenging task [11, 12], since introducing any kind of measuring equipment into the IBC channel modifies the return signal path and influences the measurement results. For accurate measurements, measuring equipment (signal generator, oscilloscope, network and spectrum analyser) should be galvanically decoupled from the IBC channel. This is usually achieved using an optical link, differential probe or, more often, connecting balun transformers between the transmitter/receiver electrodes and the rest of the measuring equipment, as in Fig. 1 [4, 13, 14].

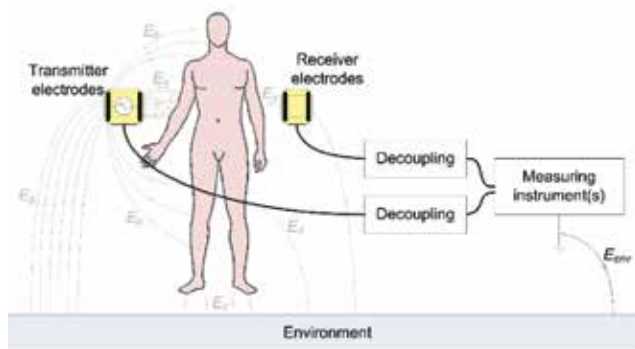


Figure 1. General capacitive IBC measurement setup using commercial equipment.

The group investigated influences of the type, size, and position of the transmitter and receiver electrodes, and the influence of the environment in a capacitive IBC channel. Several thousand *in vivo* measurements were performed on a larger number of test subjects with different anatomical characteristics, for several static and dynamic body positions in the frequency range from 100 kHz to 100 MHz. Channel gain was measured using commercial network analysers (power-line and battery powered), with and without balun transformers for decoupling. Transmission characteristics of the capacitive intrabody communication channel in all measuring combinations showed band-pass characteristics: an increase 20 dB/decade up to around 45 MHz, and a steep decrease at higher frequencies, as in Fig. 2.

Additional measurements were performed using a proprietary battery-powered transmitter for signal generation, and the battery-powered spectrum analyser for measuring the received signal power [15]. The results agree qualitatively with the previous ones.

However, it has been recently shown that the value of the capacitance between primary and secondary windings of the transformer and its symmetry with

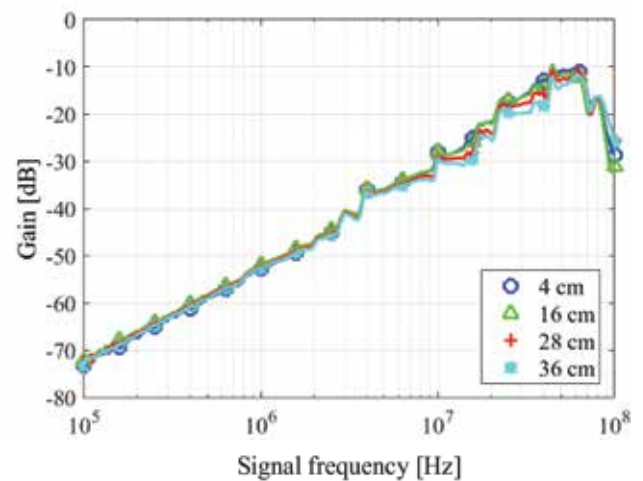


Figure 2. Capacitive IBC channel transmission characteristics measured at four transmitter-receiver distances.

respect to the ground could influence results drastically [14, 16]. Furthermore, using balun transformers and commercial equipment with 50 Ω input impedance results in higher measured gain than in a realistic IBC channel due to the improper ground isolation, and with lower gain at low frequencies due to the low frequency termination [17, 18]. Also, devices with large physical size (like commercial network and spectrum analysers) create a larger than expected return path, whether they were isolated with baluns or not, thereby increasing the measured channel gain [4, 16-18]. Therefore, for performing accurate measurements of IBC channel transmission characteristics, testing apparatuses should be of the same physical size and have the same grounding configurations as devices that will eventually be employed in IBC applications, with the corresponding matching networks between devices and the human body. In other words, measurements of any IBC channel transmission characteristics should be performed using small and independent battery-powered devices, thus bypassing the need for galvanic decoupling and providing a more realistic IBC channel.

Currently, the group is developing proprietary small battery-powered devices (signal generator and received power meter) for IBC channel characterization in a realistic communication scenario and a wider frequency range. The plan is to use them for IBC channel gain measurements for devices worn on the human body, and also for the implants.

Preliminary results of the first *in vivo* measurements of capacitive intrabody communication with implant-like devices on humans were presented in [19]. The IB2OB channel was mimicked by placing the transmitter under the armpit and taking different body positions while covering transmitter electrodes with tissue. The results agreed qualitatively to the results of the on-body channel measurements obtained using the same battery-powered equipment and baluns for decoupling as in [13, 14].

Since experiments with implanted capacitive IBC devices on living beings would be highly invasive, measurements of implantable capacitive IBC channels are usually made on human body phantoms rather than on humans. Human tissue phantoms are made by combining simple chemical substances with water for adjusting the conductivity and relative permittivity of the solution. However, it is rather difficult to produce solutions that emulate the electrical properties of human tissues in a wide range of frequencies, so a single phantom can be used at a specified frequency or in a narrow frequency band. The tissue phantom in which the in-body transmitter is placed needs to be liquid, so the distance between transmitter and receiver electrodes can be adjusted during the measurements; while outer tissues in multilayer phantoms can be semi-solid or animal skin. Receiver electrodes are placed inside the phantom for implantable to implantable channel measurements, and on the outer layer of a phantom for implantable to on-body (IB2OB) channel measurements, as in Fig. 3. Transmitter electrodes are immersed in the liquid phantom and their position can be adjusted in all three directions. The liquid phantom in Fig. 3 has conductivity similar to human muscle tissue ($7.38 \text{ mS/cm @ } 22.7^\circ\text{C}$), which is achieved adding 56 g of sodium chloride to 14 l of distilled water. The first results obtained using the aforementioned setup are promising.



Figure 3. Measurement setup for implantable to on-body channel measurements on a muscle tissue equivalent liquid phantom.

IBC channel characterization by modelling

The research group developed several types of IBC channel models of the human limbs, most recent based on anthropometric data of several persons [20] and based on Visible Human Data [21].

In [20] the safety of galvanic IBC was analysed using empirical FEM arm models based on the geometrical information of six subjects with different physiological characteristics. The weight, fat percentage, and muscle percentage for each subject were measured and geometrical dimensions for the arm model in Fig. 4 were calculated and models were developed in COMSOL 5.2 Multiphysics Software. The electric field intensity and

localized SAR were computed and, in some cases, 2010 ICNIRP safety limits were exceeded. To comply with safety standards, the use of a frequency signal of 100 – 300 kHz has been proposed for galvanic IBCs, allowing a current signal of 1–10 mA and a voltage signal of 1–2 V.

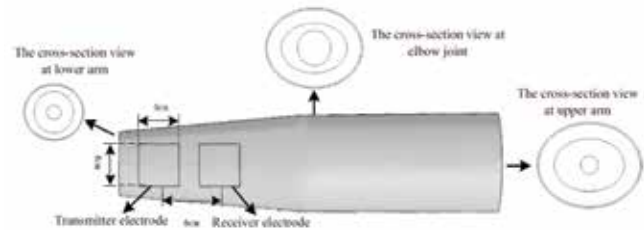


Figure 4. The empirical equivalent arm model and the electrode configurations, [20].

Visible Human Data (VHD) set [21] contains transverse anatomical images of a male taken in cross-sections 1 mm apart and showing all internal tissues. VHD images include different textures, densities, colours, and other details that are difficult to reconstruct in the 3D layer model directly, so the modelling was implemented using several software packages, such as Photoshop, Mimics, Geomagic Studio, Solidworks. The original images were firstly divided into tissue layers (skin, fat, muscle, and bone, if necessary). The outlines of each tissue were extracted automatically on every anatomical image and the contour lines of tissues were reconstructed using 3D reconstruction software, to better differentiate each layer. Contours were filled with the respective tissue and a 3D model was smoothed and divided into 3D models of each tissue. Tissue conductivity σ and permittivity ϵ , were derived from the Gabriel parametric models [22].

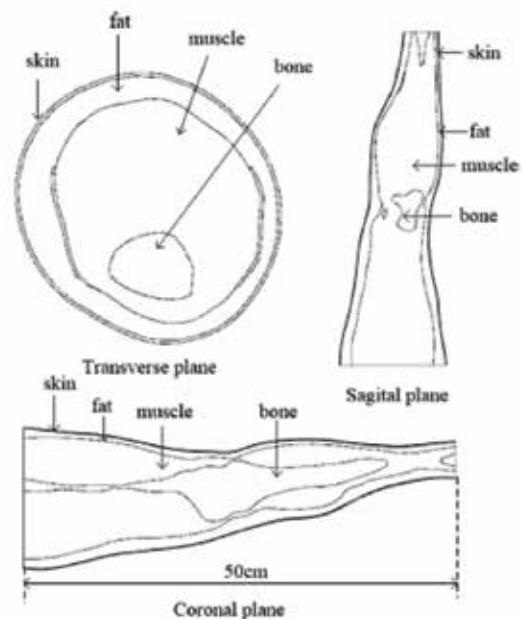


Figure 5. Human body leg model based on Visual Human Data, [23].

The numerical leg model based on Visual Human Data consisting of skin, fat, muscle, and bone layers is presented in Fig. 5, [23]. The model was used for simulation of galvanic IBC communication between implanted medical devices and external equipment in a frequency range between 10 kHz and 1 MHz, [23]. Transmitter electrodes were attached to the skin surface and the receiver electrodes were placed between the muscle and fat layers. The transmitter-receiver distance was set to 6 cm or 30 cm near the ankle, knee, and hip, respectively, e.g. in Fig. 6.

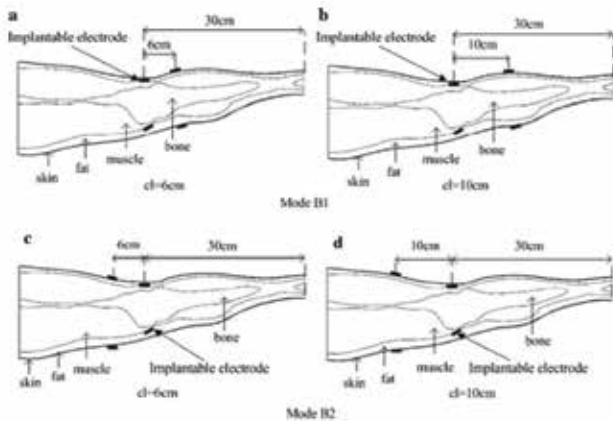


Figure 6. Several positions of electrodes near the knee, [23].

Additionally, two layer phantom models of a leg were built with tissue conductivities and permittivities chosen for 40 kHz frequency. Since at 40 kHz the conductivities of the fat and skin layers were almost the same and the influence of the bone tissue is minor, the model consisted of a muscle and a skin-fat layer. Both tissues were made by mixing agar, potassium chloride, hydroxyethyl cellulose (HEC) and distilled water. The electrical conductivity of the layer was set adjusting the quantity of potassium chloride in the mixture. Outer contours of the muscle and skin-fat layers based on the Visible Human Leg data were 3D printed and used as a mould for the mixture. After the layers of the model were produced, electrodes were placed at the same positions as in the numerical model, Fig. 7. A detailed explanation of the design, production, and verification of the phantom model can be found in the paper [24].

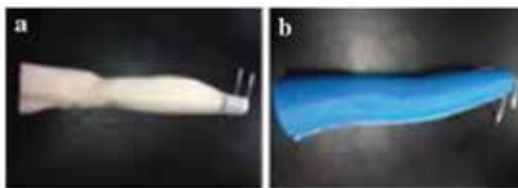


Figure 7. Phantom model, (a) muscle layer (white), (b) complete model, outer is skin-fat layer (blue) [23].

The transmission characteristics were calculated and measured for numerical and phantom models, respectively. Both models showed the same characteristics for

all electrodes positions, which proved that the simple phantom model can be used as an effective supplement to the FEM model in the design and performance test of implantable transceiver, as well as in the research of implantable channels in the future.

IBC devices

In the design of IBC devices, the design of the matching network and the choice of the optimal modulation method are important aspects.

Programmable System-on-Chip (PSoC) is a family of microcontrollers which include a CPU core and mixed-signal arrays of configurable integrated analog and digital peripherals that can be arbitrarily routed and interconnected. IBC systems based on PSoC microcontrollers were developed for low data-rate applications. Transmitters acted as signal generators and synthesized a continuous FSK (frequency shift keying) [25], BPSK (binary phase shift keying) [26], or on-off-keying (OOK) [27] modulated signals using digital to analog conversion in the microcontroller. The receivers performed the demodulation and recovering of the sent digital data. The developed systems were tested *in vivo* and successfully achieved the desired functionality, especially considering that no external components were added in the systems [25] and [26] other than the electrodes, and only two passive external components were added to the system [27], Fig. 8. Methods for increasing generated signal frequency up to several megahertz on PSoC platform will be explored and other modulation methods will be tested in order to find optimal communication requirements for PSoC platform.

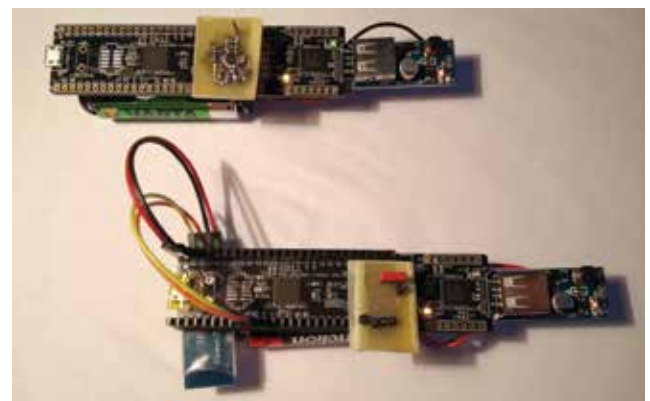


Figure 8. OOK receiver (up) and transmitter (down) on PSoC boards described in [27].

The development and improvements of the IBC interface and FPGA transceivers for galvanic IBC devices were described in papers [28-30]. In [28] field programmable gate array (FPGA, XC6SLX16) was used as a platform for testing modulation and demodulation methods in different application scenarios. Direct sequence spread spectrum (DSSS) communication

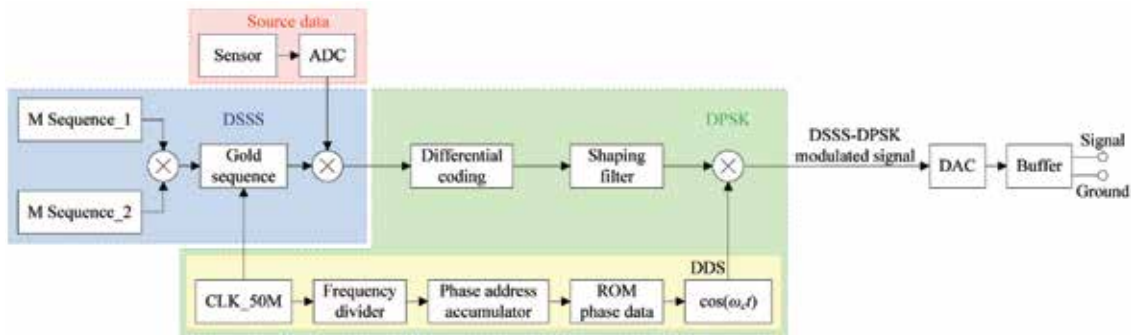


Figure 9. Block diagram of DSSS-DPSK transmitter, [27].

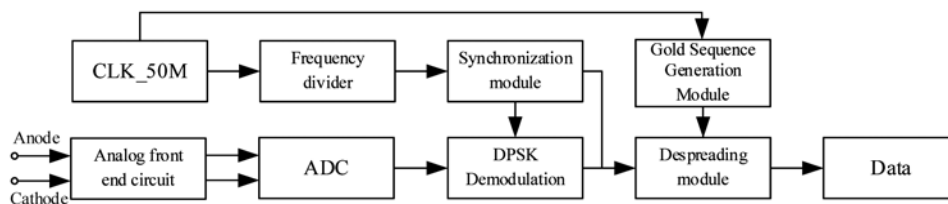


Figure 10. Block diagram of the receiver, [27].

and phase modulation were adopted to realize DSSS-differential phase shift keying (DPSK) and DPSK modulation transmission of baseband data. The block diagram of DSSS-DPSK transmitter is presented in Fig. 9. The transmitter is composed of a source module, a direct digital synthesis (DDS) module, a spread spectrum module, and a DPSK modulation module. The DSSS-DPSK signal is sent to the DAC (digital-to-analog converter) and then to the buffer. Finally, the signal is sent to the human body for transmission via transmitter signal and ground electrodes. The DPSK transmitter was also built equipped with the same peripheral circuit. The overall design of the DSSS-DPSK signal receiver is shown in Fig. 10. The main parts of the receiver are an analog front end (AFE), a DPSK demodulation module, a despreading module, and a synchronization module. The analog front end mainly preprocesses the signal that enters the receiver. The Costas loop method was employed to achieve reliable symbol recovery. *In vivo* experiments were conducted to compare the

performance of DSSS-DPSK and DPSK galvanic coupling IBC transceiver systems under the same conditions. The generated signal frequency was 2 MHz for both DSSS-DPSK and DPSK transmitters. The set channel lengths (transmitter-receiver distances) were 10 cm, 30 cm, 90 cm, and 120 cm. The influence of human activity (arm still or moving), signal-to-noise ratio (SNR), and transmission distance were tested and compared by measuring the bit error ratio. The bit error ratio (BER) was calculated dividing the number of bits received in error by the total number of bits transmitted within the same time period:

$$BER = \frac{\text{Number of bit errors}}{\text{Total number of bits}}$$

so the lower the BER value the better.

In order to test the BER performance, two PCIe-6361 data acquisition cards were used to collect the baseband data at the transmitter and the demodulated data at the

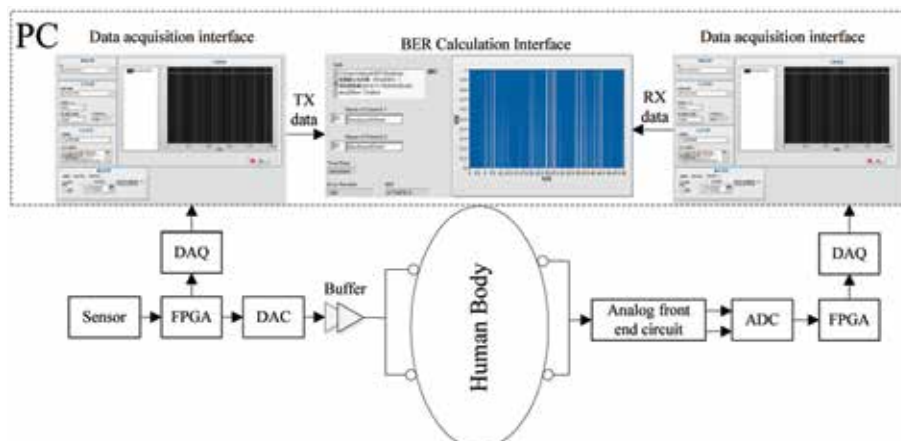


Figure 11. BER test platform

receiver, as in Fig. 11. As expected, the BER decreased as SNR improved for both cases, regardless of the body movements of the test subject, Fig. 8. BER was also lower at lower transmitter-receiver distances. It was shown that DSSS-DPSK modulation requires a lower SNR than DPSK modulation. The BER measured with DPSK transceivers was 40 times greater than with DSSS-DPSK transceivers at a transmitter-receiver distance of 30 cm and different SNR values. When changing the BER from extremely poor (1.40×10^{-1}) to excellent (1.51×10^{-6}), the SNR of DSSS-DPSK transceivers only had to be improved by 16 dB. In contrast, when the BER was changed from extremely poor (1.54×10^{-1}) to good (1.65×10^{-5}), the SNR of the DPSK method had to be improved by 25 dB. With a SNR equal to 5 dB, the BER ratio using DPSK transceivers was 7 times larger than using the DSSS-DPSK transceivers. However, DSSS-DPSK transceivers were statistically more sensitive to changes in motion status than DPSK.

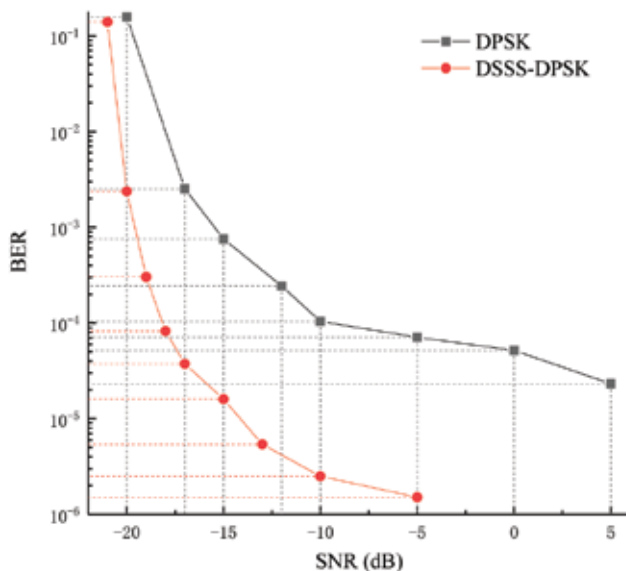


Figure 12. Average BER of motion and stationary vs. SNR for both tested modulations.

References

- [1] A. K. Teshome, B. Kibret, and D. T. H. Lai, "A Review of Implant Communication Technology in WBAN: Progress and Challenges," *IEEE Reviews in Biomedical Engineering*, vol. 12, pp. 88–99, June 2019.
- [2] D. Naranjo-Hernández, M. A. Callejón-Leblic, Ž. Lučev Vasić, M. Seyedi, and Y.-M. Gao, "Past results, present trends, and future challenges in intrabody communication," *Wireless Communications and Mobile Computing*, vol. 2018, pp. 1–39, Mar. 2018.
- [3] J. F. Zhao, X. M. Chen, B. D. Liang, and Q. X. Chen, "A review on human body communication: Signal propagation model, communication performance, and experimental issues," *Wireless Communications and Mobile Computing*, vol. 2017, pp. 1–15, Oct. 2017.
- [4] I. Čuljak, Ž. Lučev Vasić, H. Mihaldinec, and H. Džapo, "Wireless Body Sensor Communication Systems Based on UWB and IBC Technologies: State-of-the-Art and Open Challenges," *Sensors*, vol. 20, no. 12, pp. 1–33, 2020.
- [5] K. Zhang, Q. Hao, Y. Song, J. Wang, R. Huang, and Y. Liu, "Modeling and characterization of the implant intra-body communication based on capacitive coupling using a transfer function method," *Sensors*, vol. 14, no. 1, pp. 1740–1756, 2014.
- [6] M. Li, Y. Song, G. Wang, Q. Hao, and K. Zang, "Characterization of the implantable intra-body communication based on capacitive coupling by transfer function," in *2016 10th International Conference on Sensing Technology (ICST)*, pp. 1–5, Nov. 2016.
- [7] M. Li, Y. Song, Y. Hou, N. Li, Y. Jiang, M. Sulaman, and Q. Hao, "Comparable investigation of characteristics for implant intra-body communication based on galvanic and capacitive coupling," *IEEE Transactions on Biomedical Circuits and Systems*, vol. 13, pp. 1747–1758, Dec. 2019.
- [8] J. Jang and H. Yoo, "A capsule endoscope system for wide visualization field and location tracking," in *2018 IEEE Biomedical Circuits and Systems Conference (BioCAS)*, pp. 1–4, Oct 2018.
- [9] J. Jang, J. Lee, K. Lee, J. Lee, M. Kim, Y. Lee, J. Bae, and H. Yoo, "A Four-Camera VGA-Resolution Capsule Endoscope System With 80-Mb/s Body Channel Communication Transceiver and Sub-Centimeter Range Capsule Localization," *IEEE Journal of Solid-State Circuits*, vol. 54, pp. 538–549, Feb. 2019.
- [10] S. Maity, M. Nath, G. Bhattacharya, B. Chatterjee, and S. Sen, "On the safety of human body communication," *IEEE Transactions on Biomedical Engineering*, vol. 67, no. 12, pp. 3392–3402, 2020.
- [11] M. Nath, S. Maity, and S. Sen, "Towards understanding the return path capacitance in capacitive human body communication," *IEEE Transactions on Circuits and Systems II: Express Briefs*, vol. 67, pp. 1879–1883, oct 2020.
- [12] J. Zhao, W. Sun, J. Mao, Y. Huang, B. Zhao, Y. Liu, and H. Yang, "An auto loss compensation system for capacitive-coupled body channel communication," *IEEE Transactions on Biomedical Circuits and Systems*, vol. 13, pp. 756–765, Aug 2019.
- [13] Ž. Lučev, I. Krois, and M. Cifrek, "A capacitive intrabody communication channel from 100 kHz to 100 MHz," *IEEE Transactions on Instrumentation and Measurement*, vol. 61, pp. 3280–3289, Dec. 2012.
- [14] Ž. Lučev Vasić, I. Krois, and M. Cifrek, "Effect of transformer symmetry on intrabody communication channel measurements using grounded instruments," *Automatika: journal for control, measurement, electronics, computing and communications*, vol. 57, pp. 15–26, Sept. 2016.
- [15] Ž. Lučev Vasić, I. Krois, and M. Cifrek, "Measurement of the received power in a realistic intrabody communication scenario," in *World Congress on Medical Physics and Biomedical Engineering, June 7-12, 2015, Toronto, Canada* (D. A. Jaffray, ed.), (Cham), pp. 924–927, Springer International Publishing, 2015.

- [16] G. A. Álvarez-Botero, Y. K. Hernández-Gómez, C. E. Telléz, and J. F. Coronel, "Human body communication: Channel characterization issues," *IEEE Instrumentation Measurement Magazine*, vol. 22, pp. 48–53, Oct 2019.
- [17] J. Park, H. Garudadri, and P. P. Mercier, "Channel modeling of miniaturized battery-powered capacitive human body communication systems," *IEEE Transactions on Biomedical Engineering*, vol. 64, pp. 452–462, Feb. 2017.
- [18] S. Maity, M. He, M. Nath, D. Das, B. Chatterjee, and S. Sen, "BioPhysical Modeling, Characterization and Optimization of Electro-Quasistatic Human Body Communication," *IEEE Transactions on Biomedical Engineering*, vol. 66, no. 6, pp. 1791–1802, 2019.
- [19] Ž. Lučev Vasić, M. Cifrek, Y. Gao, and M. Du, "Preliminary characterization of capacitive intrabody communication channel under implantable-like conditions," in *Proc. of IEEE Instrumentation and Measurement Technology Conference (I2MTC2020)* (S. Rapuano, W. Van Moer, and D. Vasić, eds.), pp. 1–5, May 2020.
- [20] Y.-M. Gao, H.-f. Zhang, S. Lin, R.-X. Jiang, Z.-Y. Chen, Ž. Lučev Vasić, M.-I. Vai, M. Du, M. Cifrek, and S.-H. Pun, "Electrical exposure analysis of galvanic-coupled intrabody communication based on the empirical arm models," *BioMedical Engineering OnLine*, vol. 17, pp. 1–16, June 2018.
- [21] V. Spitzer, M. J. Ackerman, A. L. Scherzinger, and D. Whitlock, "The visible human male: a technical report," *Journal of the American Medical Informatics Association (JAMIA)*, vol. 3, no. 2, pp. 118–130, 1996.
- [22] S. Gabriel, R. W. Lau, and C. Gabriel, "The dielectric properties of biological tissues: III. Parametric models for the dielectric spectrum of tissues," *Physics in Medicine and Biology*, vol. 41, pp. 2271–2293, Nov. 1996.
- [23] Y.-M. Gao, Y.-T. Ye, S. Lin, Ž. Lučev Vasić, M.-I. Vai, M. Du, M. Cifrek, and S.-H. Pun, "Investigation of implantable signal transmission characteristics based on visible data of the human leg," *BioMedical Engineering OnLine*, vol. 16, no. 88, pp. 1–14, 2017.
- [24] L. Huang, Y. Gao, D. Li, Ž. Lučev Vasić, M. Cifrek, M. I. Vai, M. Du, and S. H. Pun, "A leg phantom model based on the visible human data for intra-body communication," *IEEE Journal of Electromagnetics, RF and Microwaves in Medicine and Biology*, vol. 5, no. 4, pp. 313–321, 2021.
- [25] F. Grilec, Ž. Lučev Vasić, W. Ni, Y. Gao, M. Du, and M. Cifrek, "Wireless intrabody communication sensor node realized using PSoC microcontroller," in *2016 39th International Convention on Information and Communication Technology, Electronics and Microelectronics (MIPRO)*, pp. 426–429, May 2016.
- [26] F. Grilec, A. Stanešić, Ž. Lučev Vasić, Y. Gao, M. Du, and M. Cifrek, "Single-chip intrabody communication node," in *CMBEBIH 2017: Proceedings of the International Conference on Medical and Biological Engineering 2017* (A. Badnjević, ed.), (Singapore), pp. 305–310, Springer Singapore, Mar. 2017.
- [27] A. Stanešić, Ž. Lučev Vasić, Y. Gao, M. Du, and M. Cifrek, "Integrated intrabody communication node based on OOK modulation," in *CMBEBIH 2021* (A. Badnjevic and L. Gurbeta Pokvić, eds.), (Cham), pp. 107–115, Springer International Publishing, 2021.
- [28] W. Chen, Z. Wei, Y.-M. Gao, Ž. Lučev Vasić, M. Cifrek, M.-I. Vai, M. Du, and S.-H. Pun, "Design of galvanic coupling intra-body communication transceiver using direct sequence spread spectrum technology," *IEEE Access*, vol. 8, pp. 84123–84133, 2020.
- [29] Z.-L. Wei, W.-K. Chen, M.-J. Yang, Y. Gao, Ž. Lučev Vasić, and M. Cifrek, "Design and implementation of galvanic coupling intra-body communication transceivers using differential phase shift keying," in *Proc. of IEEE Instrumentation and Measurement Technology Conference (I2MTC2020)* (S. Rapuano, W. Van Moer, and D. Vasić, eds.), pp. 1–6, May 2020.
- [30] D. Li, J. Wu, Y. Gao, M. Du, Ž. Lučev Vasić, and M. Cifrek, "A differential analog receiver front-end for galvanic-coupled human body communication," in *Proc. of IEEE Instrumentation and Measurement Technology Conference (I2MTC2020)* (S. Rapuano, W. Van Moer, and D. Vasić, eds.), pp. 1–5, May 2020.